Lithos 266–267 (2016) 202–212

Contents lists available at ScienceDirect

Lithos

journal homepage: www.elsevier.com/locate/lithos

# Geochronology and geochemistry of Late Cretaceous–Paleocene granitoids in the Sikhote-Alin Orogenic Belt: Petrogenesis and implications for the oblique subduction of the paleo-Pacific plate

Jie Tang [a,b], Wenliang Xu [a,c,*], Yaoling Niu [b,d], Feng Wang [a], Wenchun Ge [a], A.A. Sorokin [e], I.Y. Chekryzhov [f,g]

[a] College of Earth Sciences, Jilin University, Changchun 130061, China
[b] Department of Earth Sciences, Durham University, Durham DH1 3LE, UK
[c] State Key Laboratory of Geological Processes and Mineral Resources, China University of Geosciences, Wuhan 430074, China
[d] Institute of Oceanology, Chinese Academy of Sciences, Qingdao 266071, China
[e] Institute of Geology and Nature Management, Far Eastern Branch of the Russian Academy of Sciences, ul. B. Khmel'nitskogo 2, Blagoveshchensk 675000, Russia
[f] Far East Geological Institute, 159 Pr 100-let Vladivostoku, Vladivostok, Russia
[g] Engineering School, Far Eastern Federal University, 8 Sukhanova Str, Vladivostok, Russia

ARTICLE INFO

*Article history:*
Received 25 January 2016
Accepted 24 September 2016
Available online 07 October 2016

*Keywords:*
Sikhote-Alin Orogenic Belt
Late Cretaceous–Paleocene
Granitoids
Petrogenesis
Oblique subduction
Paleo-Pacific plate

ABSTRACT

We present zircon U–Pb ages, major and trace element analyses, and zircon Hf isotope data on the Late Cretaceous–Paleocene granitoids at the southern end of the Sikhote-Alin Orogenic Belt of the Russian Far East. These data are used to discuss the petrogenesis of the granitoids in the context of the paleo-Pacific subduction beneath the eastern Eurasia. Zircons from four granitoid samples give emplacement ages of ~56, ~83, ~91, and ~92 Ma. These granitoids with high $SiO_2$ (73.43–76.76 wt%) are metaluminous to weakly peraluminous (A/CNK = 0.97–1.03) and belong to the high-K calc-alkaline series ($K_2O$ = 3.75–4.95 wt%). They are all enriched in light rare earth elements (LREEs) and large ion lithophile elements (LILEs), and relatively depleted in high field strength elements (HFSEs) with striking depletion also in Ba, Sr, P and Eu. They are petrographically and geochemically consistent with being of I-type granitoids. The zircons have $\varepsilon_{Hf}$ (t) values (−0.8 to +7.6) higher than whole-rock $\varepsilon_{Hf}$ (t) values predicted from whole-rock $\varepsilon_{Nd}$ (t) (−4.1 to +0.5) in the literature. All these observations suggest that primary magmas parental to these granitoids were likely to have derived from partial melting of a juvenile lower crust accompanied by assimilation with ancient mature crust during magma ascent and evolution. A recent study illustrates that the collision of an exotic terrane carried by the paleo-Pacific plate with the continental China at ~100 Ma accreted the basement of the Chinese continental shelf (beneath East and South China Seas), and resulted in a new plate boundary of transform nature between the NNW moving paleo-Pacific plate and the eastern margin of the shelf. Our new data and analysis of existing data support this hypothesis, but we hypothesize that this transform becomes transpressional in its northern segment with oblique subduction of the paleo-Pacific plate beneath northeastern Asia as manifested by the Late Cretaceous-Paleocene granitoids in the Russian Far East-NE China (97–56 Ma) and South Korea-SW Japan (96–71 Ma). These tectonic and magmatic events took place prior to the opening of the Huanghai, Bohai and Japan seas, which are of rift-origin from continental China much later. Our study emphasizes the necessity and significance of plate tectonics reconstruction in the greater northwestern Pacific region since the Cretaceous.



## 1. Introduction

The Russian Far East and Northeast (NE) China comprise several massifs and terranes between the Siberia and North China cratons (Fig. 1a), including the Erguna, Xing'an, Songliao and Bureya–Jiamusi–Khanka massifs and the Sikhote-Alin Orogenic Belt (SAOB; Fig. 1a; Kotov et al., 2009; Li et al., 2010; Sorokin et al., 2010a; Sun et al., 2013; Wu et al., 2005; Yu et al., 2008; Zhou et al., 2011). Subduction of the paleo-Pacific plate beneath the Eurasian plate has been thought to play a predominant role in the Mesozoic-Cenozoic geology of the eastern Asian continent. However, the late Early Cretaceous-Paleocene tectonic setting of the northeastern Asian continent remains debatable. Some researchers consider that the eastern Russian Far East was in a transform contact with the paleo-Pacific plate during the time period of 130–100 Ma and in the Paleocene, but was a subduction environment in the Late Cretaceous (Gonevchuk et al., 2010; Khanchuk, 2001; Sorokin et al., 2005, 2010b). Others argue that the Russian Far East

* Corresponding author at: 2199 Jianshe Street, College of Earth Sciences, Jilin University, Changchun 130061, China.
*E-mail addresses:* tangjie_jlu@163.com (J. Tang), xuwl@jlu.edu.cn (W. Xu), yaoling.niu@foxmail.com (Y. Niu), jlu_wangfeng@jlu.edu.cn (F. Wang), gewenchun@jlu.edu.cn (W. Ge), sorokin@ascnet.ru (A.A. Sorokin), chekr2004@mail.ru (I.Y. Chekryzhov).

http://dx.doi.org/10.1016/j.lithos.2016.09.034
0024-4937/

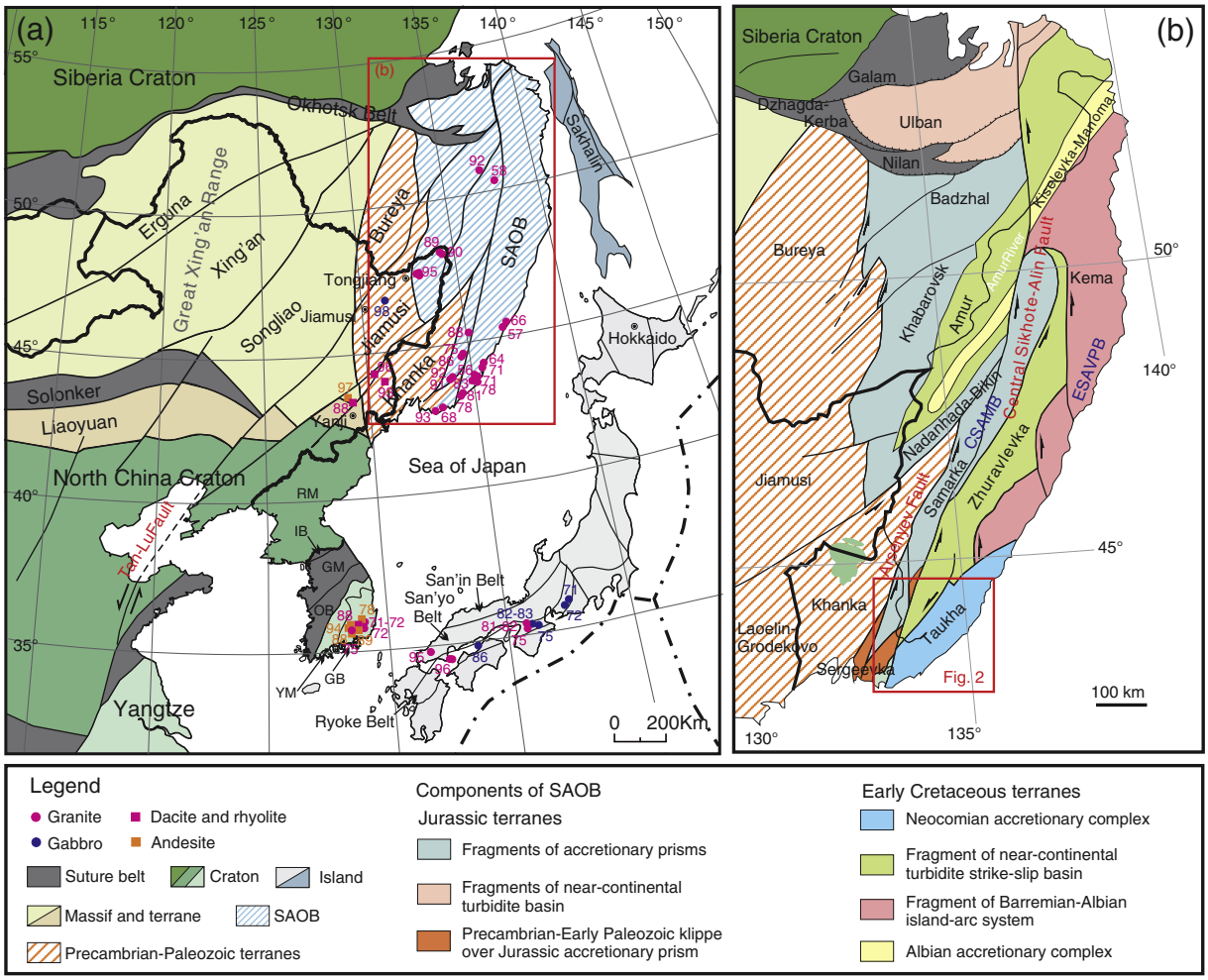


**Fig. 1.** (a) Simplified tectonic divisions of the northeastern Asian continent (modified after Barnes, 2003; Sorokin et al., 2010a; Sun et al., 2013; Wu et al., 2011) and the distribution of Late Cretaceous-Paleocene igneous rocks in the Russian Far East, NE China, SW Japan, and South Korea (Data from Herzig et al., 1998; Hwang, 2011; Jahn et al., 2015; Ji et al., 2007; Nakajima et al., 2004; Xu et al., 2013; Yu et al., 2013; Zhang et al., 2012). (b) Principal tectonostratigraphic terranes in the SAOB (modified after Jahn et al., 2015; Kruk et al., 2014). CSAMB = Central Sikhote-Alin magmatic belt; ESAVPB = East Sikhote-Alin Volcanic-Plutonic Belt; and SAOB = Sikhote-Alin Orogenic Belt.

and NE China were geologically active continental margin related to the subduction of the paleo-Pacific plate during 130–100 Ma (Faure and Natal'in, 1992; Kiminami and Imaoka, 2013; Sun et al., 2013; Wu et al., 2011; Xu et al., 2013). The exact position of the plate boundary, whether subduction or transform, is unknown.

Indeed, an analysis of Jurassic-Cretaceous granitoid distribution in space and time in the eastern continental China by Niu et al. (2015) echoes the active continental margin associated with the paleo-Pacific subduction (though not an Andean-Type), but emphasizes the magmatic termination at ~90 Ma to have resulted from the paleo-Pacific re-orientation from NW to NNW, making the eastern margin of the Chinese continental shelf in transform contact with the NNW moving paleo-Pacific plate. While this hypothesis is logical and can effectively explain the magmatic termination as the result of the trench jam and accretion of Chinese continental shelf basement. It is predictable, however, that this transform boundary developed from the prior subduction may vary locally in nature depending on the orientation and geometry of the prior contact. We thus predict that the northern extension of the transform may be transpressional and subduction may continue obliquely. Indeed, our new data and analysis of existing data show that the Late Cretaceous-Paleocene magmatism in South Korea, Southwest (SW) Japan, and the Russian Far East, NE China is most consistent with this prediction.

We undertook zircon U–Pb dating and geochemical analysis of the granitoids exposed in the southern section of the SAOB. Our samples give older ages of ~92 Ma in the interior, but younger ages at the coastal region, as young as ~56 Ma. Together with zircon U–Pb ages in the literature, the Late Cretaceous–Paleocene granitoids in the Russian Far East-NE China and South Korea-SW Japan range from 97 Ma to 56 Ma, and from 96 Ma to 71 Ma, respectively. This study supports the hypothesis of transform boundary with oblique subduction of the eastern Asian continental margin from the Late Cretaceous to the Paleocene (see below).

## 2. Geological background and sample descriptions

The SAOB represents a collage of different terranes (Fig. 1b), whose formation was closely related to the paleo-Pacific plate subduction (Malinovsky and Golozubov, 2011). The SAOB lies to the east of the late-Precambrian massifs – Bureya, Jiamusi and Khanka (Fig. 1). As shown in Fig. 1b, the SAOB is made up of several Mesozoic tectonostratigraphic terranes: the Jurassic Samarka, Nadanhada-Bikin, Khabarovsk, Badzhal, Ulban and Sergeevka terranes; the Early Cretaceous Taukha, Zhuravlevka-Amur, Kema and Kiselevka-Manoma terranes (Fig. 1b; Jahn et al., 2015; Kruk et al., 2014).

A distinctive feature of the SAOB is that it is broken by a system of sinistral strike-slip faults, the most striking being the Central Sikhote-Alin Fault (Figs. 1b and 2) with a displacement of ca. 200 km. The Fault was most active in the Early Cretaceous, and became inactive in the Late Cretaceous (Utkin, 1980). The Mesozoic-Cenozoic magmatism

in the SAOB mainly occurred in the Central Sikhote-Alin magmatic belt (CSAMB) and the East Sikhote-Alin Volcanic-Plutonic Belt (ESAVPB). The CSAMB includes many granitoid plutons and small volumes of basalt and andesite in the Zhuravlevka, Samarka and Nadanhada terranes (Simanenko et al., 2002). They were mostly emplaced in the Early Cretaceous and rarely in the Late Cretaceous to early Cenozoic (Jahn et al., 2015). The ESAVPB comprises a large volume of volcanic rocks (including basalt, andesite, and rhyolite) and numerous granitoid plutons in the Kema and Taukha terranes, which were emplaced in the Late Cretaceous to Middle Paleogene (Jahn et al., 2015).

In this study, granitoid samples 14RF34, 14RF35, and 14RF37 are collected from the Samarka and Taukha terranes in the southern section of the SAOB (Figs. 1b, 2). Note that the sample number, such as 14RF37, is a location number and in the case of more than one sample analyzed from a given location, the samples are further suffixed, e.g., 14RF37-1 and 14RF37-6.

Sample 14RF34 is a monzogranite collected from an intrusion ~20 km east of Olga Town (Fig. 2; 43°43′44″N, 135°14′24″E). It is pink, medium-grained (Fig. 3a), and consists of quartz (~30%), plagioclase (~35%), orthoclase (~30%), biotite (~3%), and accessory minerals (~2%) including zircon, apatite, and magnetite.

Sample 14RF35 is a monzogranite collected from an intrusion ~12 km northeast of Valentin (Fig. 2; 43°09′50″N, 134°26′20″E). It is medium-grained (Fig. 3b), and consists of quartz (~29%), plagioclase (~27%), orthoclase (~40%), biotite (~2%), and accessory minerals (~ 2%), including zircon, apatite, and magnetite.

Sample 14RF37 is a syenogranite collected from an intrusion ~20 km north of Benevskoye (Fig. 2; 43°28′49″N, 133°47′34″E). The syenogranite samples from different locations show varying grain size. Samples 14RF37-1, -2, -3, -4, and-5 are medium-grained (Fig. 3c), whereas samples 14RF37-6, -7, -8, and -9 are coarse-grained (Fig. 3d). However, all the samples have similar modal mineralogy, i.e., quartz (~30%), plagioclase (~16%), orthoclase (~50%), biotite (~2%), and accessory minerals (~2%) including zircon, titanite, apatite and magnetite.

## 3. Analytical methods

### 3.1. Zircon U–Pb dating

Zircons were separated from whole-rock samples using the conventional heavy liquid and magnetic techniques before handpicked under a binocular microscope, at the Institute of Geology and Nature Management, Far Eastern Branch of the Russian Academy of Sciences, Blagoveshchensk, Russia. The handpicked zircons were examined under transmitted and reflected light with an optical microscope. To reveal their internal structures, cathodoluminescence (CL) images were obtained using a JEOL scanning electron microscope housed at the State Key Laboratory of Geological Processes and Mineral Resources, China University of Geosciences, Wuhan (CUGW). Spots on zircons for analysis were chosen using the CL images. Zircon U–Pb analysis was done using an Agilent 7500a ICP–MS equipped with a 193 nm laser at CUGW. The zircon 91500 was used as an external standard for age calibration, and the NIST SRM 610 silicate glass was applied for instrument optimization. The laser spot size was set to be 32 μm during the analysis. The instrumental conditions and analytical details are given in Yuan et al. (2004). The ICPMSDataCal (Ver. 6.7; Liu et al., 2008, 2010) and

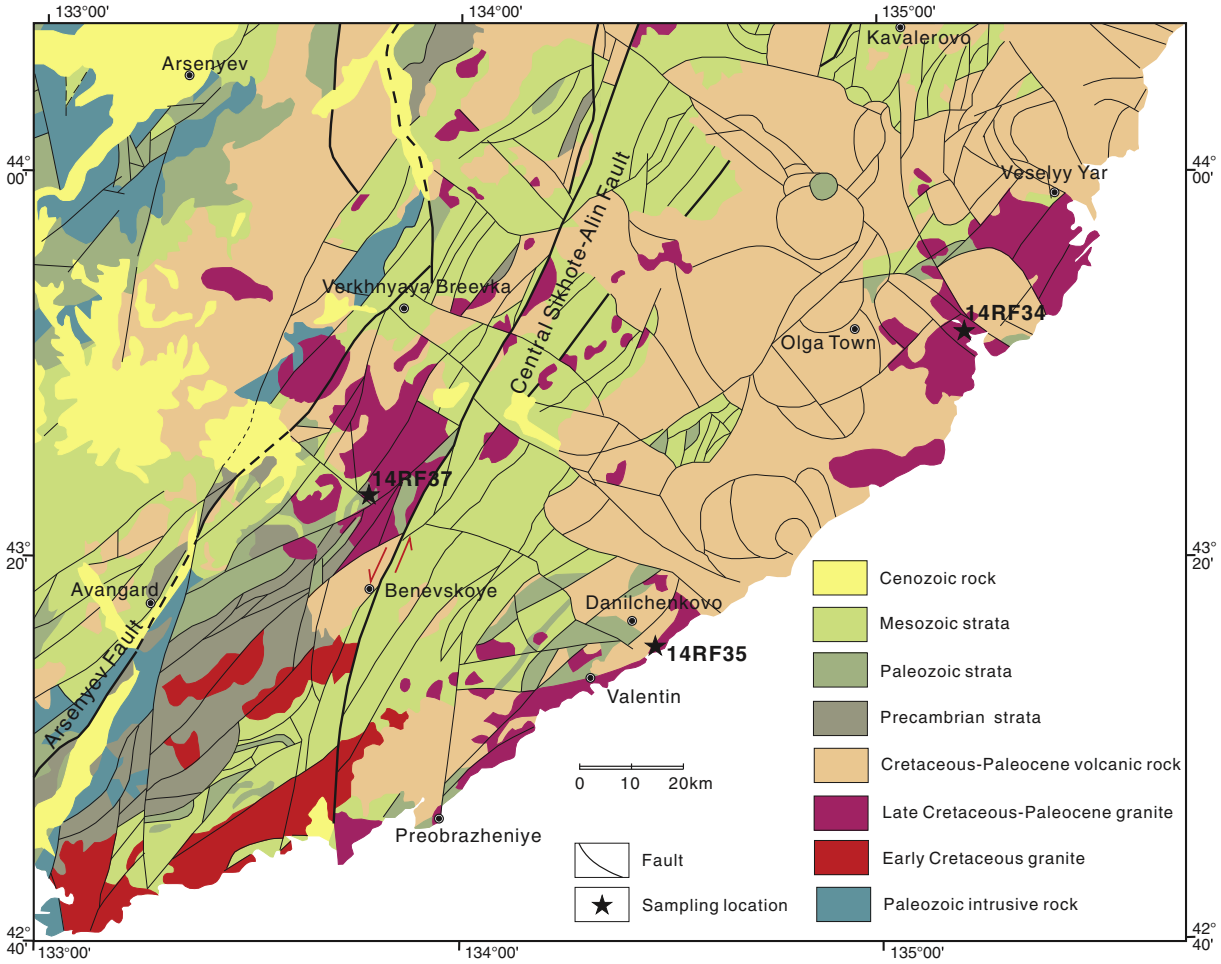


**Fig. 2.** Detailed geological map of the study area in the southern section of the Sikhote-Alin Orogenic Belt (after 1:1,000,000 geological map of Russian Far East).

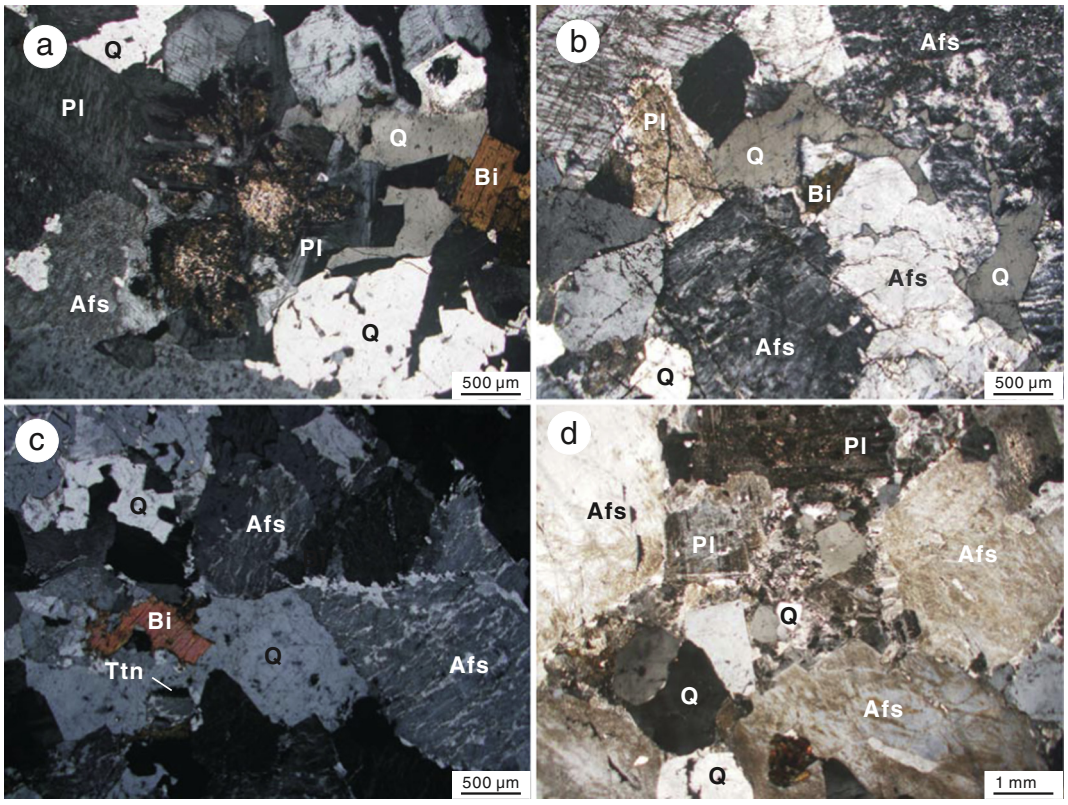


**Fig. 3.** Photomicrographs (crossed polarized light) showing typical textures of granitoid samples of this study. (a) Monzogranite (sample 14RF34–1); (b) Monzogranite (sample 14RF35–1); (c) Syenogranite (sample 14RF37–1); (d) Syenogranite (sample 14RF37–6). Afs = alkali feldspar; Bi = biotite; Pl = plagioclase; Q = quartz; and Ttn = titanite.

Isoplot (Ver. 3.0; Ludwig, 2003) programs were used for data reduction. Correction for common Pb was made following Anderson (2002). Errors on individual analyses by LA–ICP–MS are quoted at the 1σ level, while errors on pooled ages are quoted at the 95% (2σ) confidence level. The age data are given in Supplementary Table 1.

### 3.2. Major and trace element analysis

Bulk-rock samples were analyzed for major elements using XRF at the Institute of Geology and Nature Management, Far East Branch of the Russian Academy of Sciences, Blagoveshchensk, Russia and for trace elements using ICP–MS at the Institute of Tectonics and Geophysics, Far East Branch of the Russian Academy of Sciences, Khabarovsk, Russia. The precision of analyses for major and trace elements was 3–10%. The detailed analytical procedures are given in Sorokin et al. (2009). The data are given in Supplementary Table 2.

### 3.3. Hf isotope analysis

In situ zircon Hf isotope analysis was conducted using a Neptune Plus MC-ICP-MS (Thermo Fisher Scientific, Germany) in combination with a 193 nm laser at the Institute of Geology and Geophysics, Chinese Academy of Sciences, Beijing, China (IGGCAS). The operating conditions for the laser ablation system and the MC–ICP–MS instrument, as well as the analytical details are given in Wu et al. (2006). The present-day chondritic ratios of $^{176}Hf/^{177}Hf = 0.282785$ and $^{176}Lu/^{177}Hf = 0.0336$ (Bouvier et al., 2008) were adopted to calculate $\varepsilon_{Hf}$ (t) values. Hf model ages were calculated as described in the literature (e.g., Amelin et al., 2000; Griffin et al., 2000; Nowell et al., 1998). The Hf isotope data are given in Supplementary Table 3.

## 4. Analytical results

### 4.1. Zircon U–Pb dating

The zircons selected for analysis are euhedral–subhedral and display oscillatory zoning (Supplementary Fig. 1), consistent with being of magmatic origin (Koschek, 1993; Pupin, 1980).

For sample 14RF34–1 (monzogranite), twenty-seven analyses yield two groups of weighted mean $^{206}Pb/^{238}U$ ages of 56 ± 1 Ma (MSWD = 2.1, n = 18) and 63 ± 1 Ma (MSWD = 0.22, n = 6) (Fig. 4a), with further three zircons yielding ages of ~70 Ma (n = 2) and ~2640 Ma (n = 1) (Supplementary Table 1). The youngest age of 56 Ma is considered to represent the crystallization age of the monzogranite (i.e., Paleocene). The older zircon grains with $^{206}Pb/^{238}U$ ages of ~63, ~70, and ~2640 Ma are likely captured zircon crystals entrained by the monzogranite. However, these older grains cannot be distinguished from those of the ~56 Ma crystals on CL images (Supplementary Fig. 1).

For sample 14RF35-1 (monzogranite), the $^{206}Pb/^{238}U$ ages of 24 analyses range from 86 (±1) to 80 (±2) Ma, yielding a weighted mean $^{206}Pb/^{238}U$ age of 83 ± 1 Ma (MSWD = 1.8) (Fig. 4b), which is interpreted to represent the crystallization age of the monzogranite (i.e., Late Cretaceous).

For sample 14RF37-1 (syenogranite), twenty-one analyses yield a weighted mean $^{206}Pb/^{238}U$ age of 91 ± 1 Ma (MSWD = 1.9) (Fig. 4c) except for one zircon crystal that gives an age of 462 ± 4 Ma (Supplementary Table 1). The 91 Ma age is considered to represent the crystallization age of the syenogranite (i.e., Late Cretaceous), whereas the 462 ± 4 Ma age is interpreted to be the crystallization age of captured zircons entrained by the syenogranite.

For sample 14RF37-6 (syenogranite), 23 analyses give $^{206}Pb/^{238}U$ ages ranging from 93 (±1) to 91 (±2) Ma, yielding a weighted mean

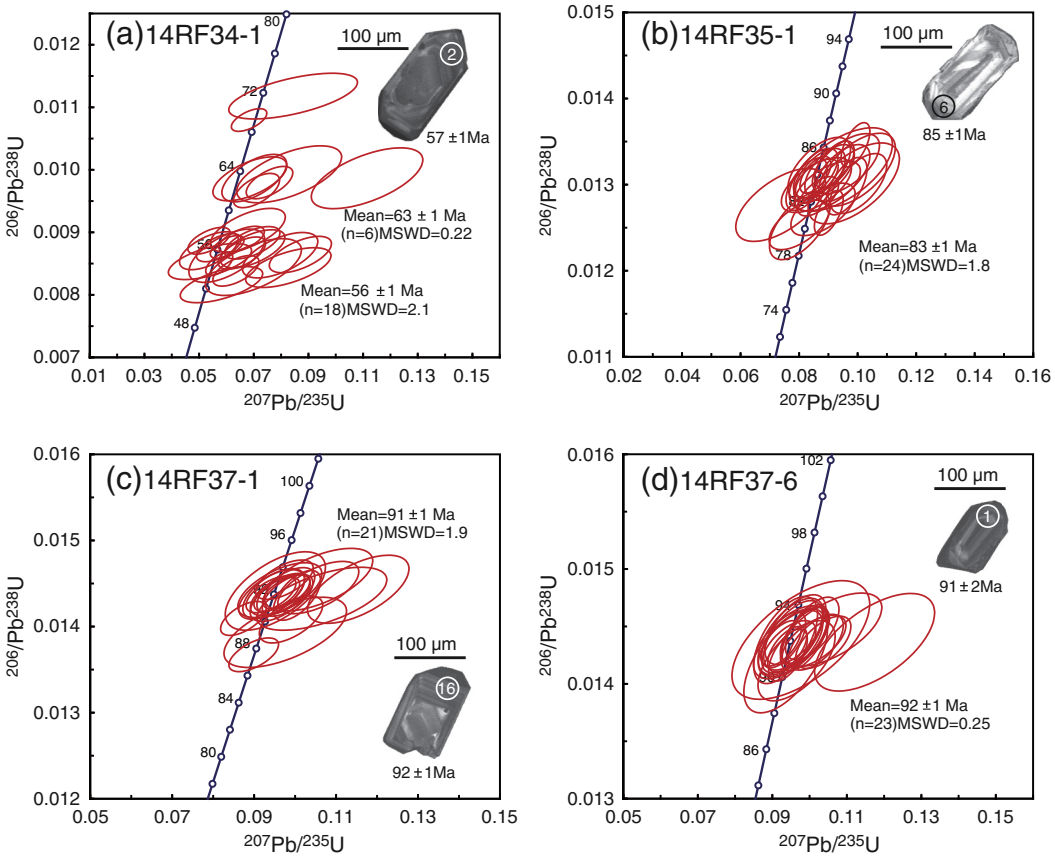


**Fig. 4.** Zircon U–Pb concordia diagrams and the representative zircon Cathodoluminescence (CL) images for the Late Cretaceous–Paleocene granitoids within the southern section of the Sikhote-Alin Orogenic Belt.

$^{206}Pb/^{238}U$ age of 92 ± 1 Ma (MSWD = 0.25) (Fig. 4d), which is interpreted to represent the crystallization age of the syenogranite (i.e., Late Cretaceous).

These age data indicate the Late Cretaceous–Paleocene granitoid magmatism in the southern section of the SAOB.

### 4.2. Geochemistry

#### 4.2.1. Major elements

The Late Cretaceous–Paleocene granitoids in the SAOB have similar major element compositions, i.e., $SiO_2$ = 73.43–76.76 wt%, total $Fe_2O_3$ ($TFe_2O_3$) = 1.42–2.37 wt%, $Al_2O_3$ = 12.22–13.48 wt%, and $Na_2O + K_2O$ = 8.34–9.02 wt% (Supplementary Table 2). These granitoids are classified as subalkaline series in the total alkalis versus $SiO_2$ (TAS) diagram (Fig. 5a). On the $K_2O$ versus $SiO_2$ variation diagram (Fig. 5b), they fall in the high-K calc-alkaline series. Their A/CNK values range from 0.97 to 1.03, indicating a transitional character from metaluminous to weakly peraluminous on an A/NK versus A/CNK diagram (Fig. 5c).

These geochemical characteristics of the Late Cretaceous–Paleocene granitoids are similar to those of the coeval intermediate–acidic igneous rocks in the literature from the SAOB (Jahn et al., 2015) and NE China (Fig. 5; Ji et al., 2007; Xu et al., 2013; Yu et al., 2013).

#### 4.2.2. Trace elements

The 83 and 56 Ma monzogranites (14RF34 and 14RF35) are enriched in light rare earth elements (LREEs) and relatively depleted in heavy rare earth elements (HREEs) ($[La/Yb]_N$ = 5.49–12.1) with negative Eu anomalies ($Eu/Eu^*$ = 0.25–0.51) (Fig. 6a). On the primitive-mantle-normalized trace element spidergram these rocks are enriched in large ion lithophile elements (LILEs; e.g., Rb and K) and depleted in high field strength elements (HFSEs) such as Nb, Ta, and Ti (Fig. 6b).

The 91 Ma medium-grained (14RF37-1, -2, -3, -4, and -5) and 92 Ma coarse-grained (14RF37-6, -7, -8, and -9) syenogranites from the same intrusion are enriched in LREEs and LILEs, and depleted in HREEs and HFSEs (Fig. 6). However, compared with the coarse-grained syenogranites ($[La/Yb]_N$ = 15.79–18.89 and $Eu/Eu^*$ = 0.12–0.17), the medium-grained syenogranites have flatter REE patterns ($[La/Yb]_N$ = 3.08–5.30) and more pronounced negative Eu anomalies ($Eu/Eu^*$ = 0.05–0.07). The medium-grained syenogranites also have lower Ba (25.1–45.8 ppm) and Sr (12.2–17.5 ppm) than the coarse-grained syenogranites (Ba = 132–150 ppm and Sr = 58.5–63.8 ppm) (Fig. 6).

### 4.3. Zircon Hf isotopes

Some zircon U–Pb dated spots on samples 14RF34-1, 14RF35-1, 14RF37-1, and 14RF37-6 were analyzed for in situ Hf isotopes (Supplementary Table 3).

The $^{176}Hf/^{177}Hf$ ratios for the ~56 Ma zircons in 14RF34-1 vary from 0.282807 to 0.282944. Their $\varepsilon_{Hf}$ (t) values and two-stage model ages ($T_{DM2}$) range from +2.4 to +7.1 and from 976 to 672 Ma, respectively. The ~63 Ma and ~69 Ma captured zircons in this same sample have $^{176}Hf/^{177}Hf$ ratios of 0.282864–0.282900, $\varepsilon_{Hf}$ (t) values of +4.6 to +5.8, and two-stage model ages ($T_{DM2}$) of 843–763 Ma (Fig. 7a and b; Supplementary Table 3). The $\varepsilon_{Hf}$ (t) value for the 2640 Ma zircon is +0.8 (Supplementary Table 3).

The $^{176}Hf/^{177}Hf$ ratios for the ~83 Ma zircons in 14RF35-1 vary from 0.282700 to 0.282818. Their $\varepsilon_{Hf}$ (t) values and $T_{DM2}$ ages range from −0.8 to +3.4 and from 1204 to 935 Ma, respectively (Fig. 7a and b; Supplementary Table 3).

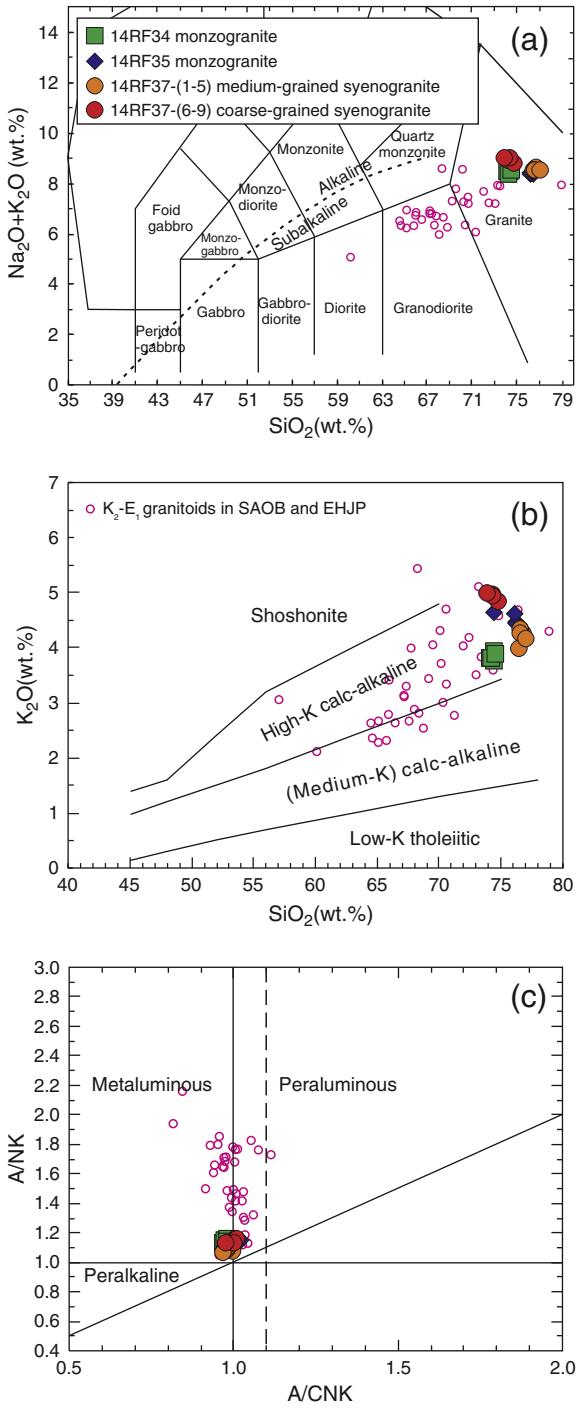


**Fig. 5.** Plots of $SiO_2$ versus $Na_2O + K_2O$, $SiO_2$ versus $K_2O$, and A/CNK [molar $Al_2O_3/(CaO + K_2O + Na_2O)$] versus A/NK [molar $Al_2O_3/(K_2O + Na_2O)$] for the Late Cretaceous–Paleocene granitoids within the southern section of the Sikhote-Alin Orogenic Belt (SAOB). The field boundaries in the three types of diagrams are from Irvine and Baragar (1971), Peccerillo and Taylor (1976), and Maniar and Piccoli (1989), respectively. Our samples are highly evolved with $SiO_2 > 73$ wt%. For comparison, plotted also are the literature data (open pink circles) on the coeval granitoids from the SAOB and the adjacent Eastern Heilongjiang-Jilin Provinces (EHJP) (Jahn et al., 2015; Yu et al., 2013). (For interpretation of the references to color in this figure legend, the reader is referred to the web version of this article.)

The $^{176}Hf/^{177}Hf$ ratios for the ~91 Ma zircons in 14RF37-1 and ~92 Ma zircons in 14RF37-6 vary from 0.282828 to 0.282935. Their $\varepsilon_{Hf}(t)$ values and $T_{DM2}$ ages range from +3.9 to +7.6 and from 909 to 669 Ma, respectively (Fig. 7a and b; Supplementary Table 3).

The Hf isotopic compositions of these selected zircons indicate that the majority of the analyzed zircons have $\varepsilon_{Hf}(t) > 0$.

## 5. Discussion

### 5.1. Late Cretaceous–Paleocene magmatic events in the Sikhote-Alin Orogenic Belt

We consider the youngest ages or age populations to represent the crystallization timing of the plutons, whereas the older ages to represent the crystallization times of captured zircons entrained by the plutonic magmatism. The age spectrum of ~56, ~83, ~ 91 and ~92 Ma indicate the long-lasting Late Cretaceous–Paleocene magmatic activity in the southern section of the SAOB. The zircons with ages of ~462 and ~2640 Ma are best interpreted as captured zircons of ancient geological events.

The Late Cretaceous–Paleocene magmatism is not restricted in the southern section of the SAOB, but is widespread in other parts of the eastern Asian continental margin (Fig. 1a). Although igneous rocks of the eastern Asian continental margin have been dated using various methods, we compiled only the ages of <~100 Ma obtained using zircon U-Pb method. A recent study by Jahn et al. (2015) reported similar LA-ICP-MS zircon U-Pb ages of granitoids in the SAOB. The granitic rocks from the southeastern coastal areas of the SAOB were emplaced in the Late Cretaceous to Paleocene (83–57 Ma). The granitoids that occur along, or close to, the Central Sikhote-Alin Fault zone were emplaced in the Late Cretaceous (93–68 Ma). The granitoids in the northern part of the SAOB were emplaced from 92 and 58 Ma. In NE China, the Late Cretaceous magmatism is only found in Yanji and Tongjiang areas of the eastern Heilongjiang-Jilin provinces (EHJP; Fig. 1a). The formation ages of the granitoids in Tongjiang area range from 95 Ma to 89 Ma (LA-ICP-MS zircon U-Pb ages, Yu et al., 2013), and the andesite and dacite in the Yanji area were emplaced from 97 Ma to 88 Ma (LA-ICP-MS zircon U-Pb ages; Ji et al., 2007; Xu et al., 2013). Taken together, the Late Cretaceous–Paleocene igneous rocks in the Russian Far East and NE China were formed in a long time period of ~40 Myrs (i.e., 97–56 Ma), and those with younger ages (83–56 Ma) are restricted to the coastal area.

Moreover, the Late Cretaceous plutons are widespread in other parts of the eastern Asian continental margin. SIMS zircon U–Pb analyses indicate that andesitic and rhyolitic rocks from the Yucheon Group in the Gyeongsang Basin (GB) of South Korea reflect a ~20 Myrs of volcanic activity (94.4–78.4 Ma) with related granitoids of ~72 Ma in the Gyeongsang Basin (Fig. 1a; Zhang et al., 2012). The SHRIMP zircon U–Pb ages of both host granite and mafic magmatic enclaves in the Gyeongsang Basin are ~75 Ma (Hwang, 2011). Additionally, SHRIMP zircon U-Pb ages of the mafic rocks occurring either as dykes and pillow lavas set in the granitic matrix or as separate bodies of gabbroic cumulate from the Ryoke Belt in SW Japan are in the range of 86–71 Ma (Nakajima et al., 2004). The granitoids in the Ryoke Belt have Late Cretaceous zircon U-Pb isotopic crystallization ages of 96–75 Ma (Fig. 1a; Herzig et al., 1998). The Hobenzan pluton containing tonalite and granitoids was emplaced at ~95 Ma in the San'yo Belt in SW Japan (LA-ICP-MS U–Pb zircon ages, Imaoka et al., 2014). Thus, the granitoid magmatism in South Korea and SW Japan occurred in the ~25 Myrs time period of 96–71 Ma (Late Cretaceous) with no younger Paleocene magmatism reported.

On the basis of statistics of literature age data of granitoids in the Mesozoic eastern China by Niu et al. (2015), the Late Cretaceous granites in South China were emplaced in the time frame of 100–90 Ma only in the coastal areas of Zhejiang and Fujian provinces. In summary, the youngest zircon U-Pb ages of the Late Cretaceous–Paleocene magmatism in South China, South Korea and SW Japan, and Russian Far East and NE China (from south to north) are ~90 Ma, ~71 Ma, and ~56 Ma, respectively. These data show that the Late Cretaceous–Paleocene magmatism in the eastern Asian continental margin ceased gradually from south to north.

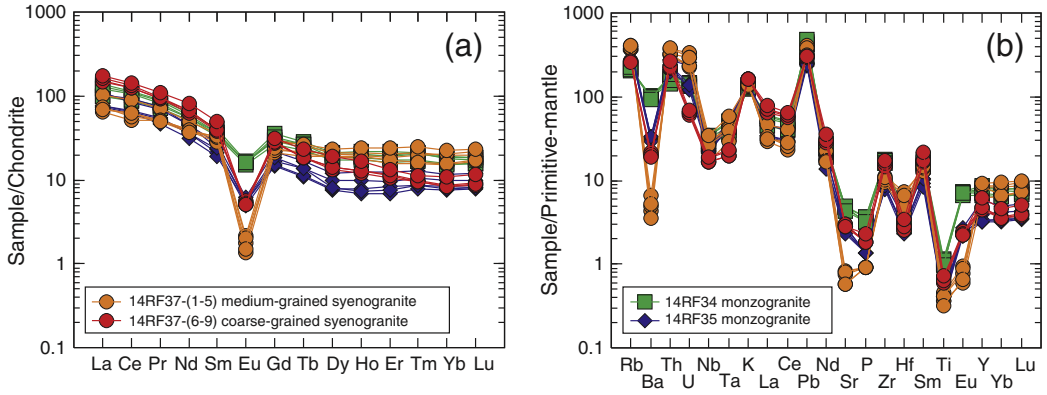


**Fig. 6.** (a) Chondrite-normalized REE and (b) primitive-mantle-normalized trace element variation diagrams for the Late Cretaceous–Paleocene granitoids in the southern section of the Sikhote-Alin Orogenic Belt. Chondrite and primitive mantle values are from Boynton (1984) and Sun and McDonough (1989), respectively.

### 5.2. Petrogenesis of Late Cretaceous–Paleocene granitoids

Our Late Cretaceous–Paleocene granitoid samples contain >95% feldspar and quartz, with minor biotite being the only mafic mineral (<3%, Fig. 3). They do not have typical peraluminous minerals (e.g., muscovite, garnet and cordierite) and high temperature anhydrous minerals (e.g., pyroxene and fayalite) (Fig. 3). Furthermore, combined with the literature data (Jahn et al., 2015), the Late Cretaceous–Paleocene granitoids in the southern section of the SAOB are mainly metaluminous with all the samples having A/CNK < 1.1, suggesting these granitoids being I-type granites (Chappell, 1999; Chappell and White, 1992, 2001). Additionally, these granitoids have striking depletions in Ba, Sr, P, Ti and Eu (Fig. 6b), which is consistent with their high $SiO_2$ as a result of significant fractional crystallization. The magmatic differentiation is more straightforward for the syenogranite (Sample 14RF37) with a relatively large range of $SiO_2$. The obvious negative correlations between $SiO_2$ and Eu, Sr, and P of Sample 14RF37 (Supplementary Table 2; Wilson, 1991) suggest the significance of plagioclase and apatite fractionation. The coeval granitoids in the SAOB and EHJP are also of I-type and have undergone significant fractional crystallization (Fig. 5; Jahn et al., 2015; Yu et al., 2013).

The new zircon $\varepsilon_{Hf}(t)$ values (−0.8 to +7.6) of this study and the values (−2.5 to 15.5) in the literature for the granitoids of 92–57 Ma in the SAOB (Jahn et al., 2015) are relatively uniform (Fig. 7b). They are all indicative of significant mantle or juvenile lower crust contribution towards the petrogenesis of these granitoids because melting of mature continental crust would produce granitoids with $\varepsilon_{Hf}(t) < 0$. Although it is convenient to ascribe the mantle-like isotopic characteristics to mantle peridotite melting for the petrogenesis of felsic magmas because wet mantle peridotite melting could produce high-Mg andesitic melts (Hirose, 1997; Kushiro et al., 1968; O'Hara, 1965), the amount of melt produced this way is too tiny to form the voluminous granitoids (Niu, 2005; Niu et al., 2013). It is also possible that granitoid melts could be formed by fractional crystallization of basaltic magmas, but again the classic volume problem remains against this possibility for the widespread and volumetrically significant granitoids (see Chappell et al., 2012; Zen, 1986). The presence of minor Maastrichtian–Paleocene basalt (of unknown age) in the SAOB (Grebennikov and Popov, 2014) cannot be used as evidence for this mechanism.

Furthermore, the SAOB is in direct contact with the paleo-Pacific plate in the Late Cretaceous-Paleocene, where island arc basalts (IAB) could be produced. However, characteristically, IAB have elevated abundances of Sr (Elliott, 2003) and plagioclase-dominated crystallization is ineffective in overcoming the variably large positive Sr anomalies ($Sr/Sr^* \gg 1$; see Fig. 4 in Niu et al., 2013), yet the 97–56 Ma SAOB granitoids have negative Sr anomalies. These observations effectively rule out the possibility of the origin due to fractional crystallization of basaltic magmas. The 97–56 Ma SAOB granitoids do not have adakitic characteristics (Fig. 6), also excluding that they were derived from a juvenile oceanic crust (subducted slab). These granitoids have typical "continental signature", e.g., enriched in LREE and LILE, depleted in HFSE. Together with their mantle-like isotopic characteristics, we consider that the magmas parental to these granitoids were derived from partial melting of juvenile lower continental crust. The heat source for crustal melting could be the underplated mantle-derived basaltic magmas.

It is worth noting that the whole-rock $\varepsilon_{Nd}(t)$ values for these granitoids range from −4.1 to +0.5. These values are equivalent to $\varepsilon_{Hf}(t) = -5.15$ to +1.99 in terms of terrestrial array ($\varepsilon_{Hf} = 1.55 \times \varepsilon_{Nd} + 1.21$; Vervoort et al., 2011), and are significantly lower than their zircon $\varepsilon_{Hf}(t)$ values (−2.5 to 15.5) (Fig. 7; Jahn et al., 2015). Zircon $\varepsilon_{Hf}(t)$ values would record the isotopic composition of the evolving magma at the time of zircon crystallization (Jahn et al., 2015), whereas the whole-rock $\varepsilon_{Nd}(t)$ (or $\varepsilon_{Hf}(t)$) values record the average isotopic composition of the whole evolving magma. Hence, the gap between whole-rock Nd and zircon Hf isotopes is best explained as resulting from assimilation of ancient crustal material after zircon crystallization. The corresponding whole-rock Hf isotope data are needed to test our explanation.

In summary, the magmas parental to the Late Cretaceous-Paleocene granitoids were derived from partial melting of a juvenile lower continental crust accompanied by assimilation with ancient crustal material during magma ascent and evolution.

### 5.3. Late Mesozoic-early Cenozoic plate tectonics reconstruction of the eastern Asian continental margin

It is generally considered that the Mesozoic granitoid magmatism in the eastern continental Asia was associated with the paleo-Pacific plate subduction and the spatial-temporal distribution of the granitoids has thus been used to discuss the tectonic evolution of the paleo-Pacific plate (Niu et al., 2015; Wu et al., 2011; Xu et al., 2013). It is thus necessary to reconstruct the late Mesozoic-early Cenozoic tectonics of the eastern Asian continental margin. The primary task is to determine the tectonic relationship among the continental China, the Japanese Islands and the Korean Peninsula. This is beyond the scope of this paper, but our data offer us important perspectives for future efforts and refinement.

The Sea of Japan opened in the Miocene and has been explained as being caused by back arc spreading due to Pacific plate subduction (Otofuji et al., 1985). Consequently, the Japanese Islands were suggested to be a continental fragment rifted from the Asian continental margin (Barnes, 2003; Lee et al., 1999). The paleomagnetic data have been used to suggest that the landmass of SW Japan underwent clockwise rotation and thus must have separated from the Russian Far East (Otofuji, 1996). However, this interpretation is inconsistent with the basement

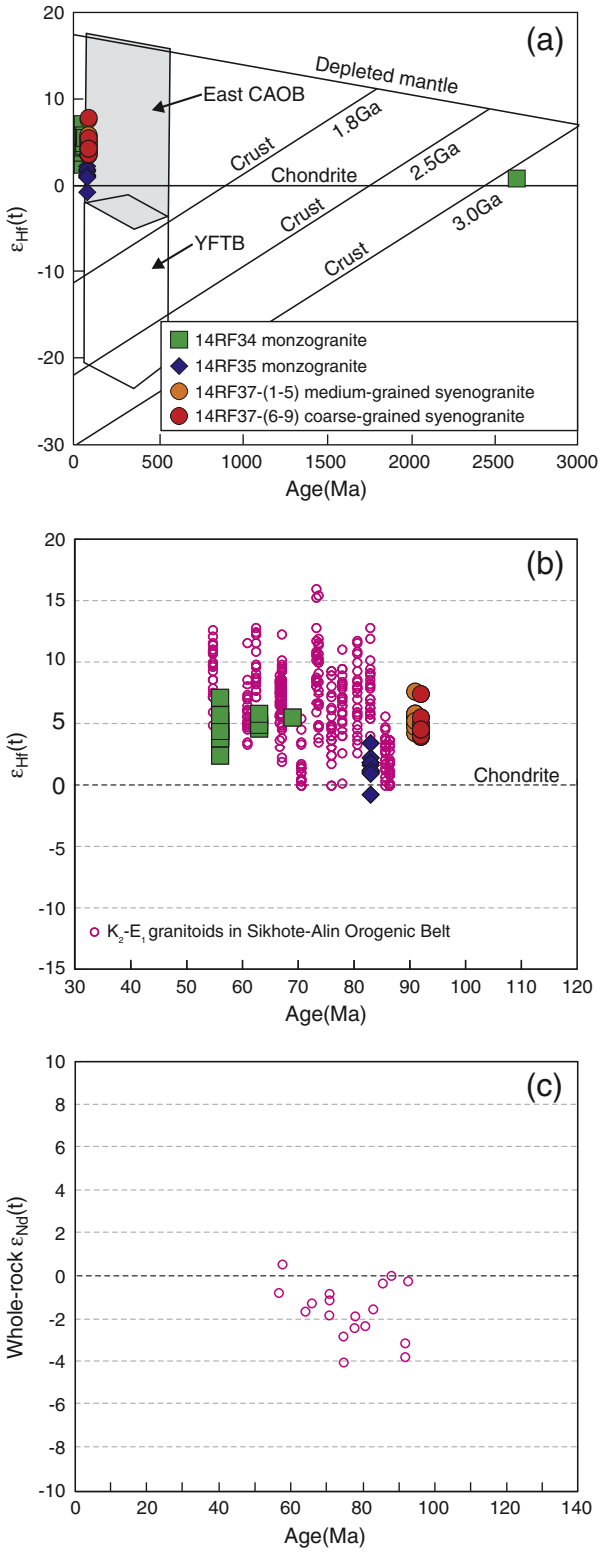


**Fig. 7.** (a) and (b) Co-variations between zircon $\varepsilon_{Hf}$ (t) values and zircon ages and (c) co-variation between whole-rock $\varepsilon_{Nd}$ (t) values and zircon ages for the Late Cretaceous–Paleocene granitoids in the Sikhote-Alin Orogenic Belt; CAOB = Central Asian Orogenic Belt; YFTB = Yanshan Fold and Thrust Belt (Yang et al., 2006); The pink open circles, as in Fig. 7, represent the coeval granitoids in the Sikhote-Alin Orogenic Belt (Jahn et al., 2015). (For interpretation of the references to color in this figure legend, the reader is referred to the web version of this article.)

rocks having the affinity with the Cathaysia Block in South China (vs. the anticipated North China and Russian Far East). The age spectra of detrital zircons of the Jurassic clastic rocks of the Mino-Tanba accretionary complex in SW Japan suggest that the exposures of middle Paleozoic to early Mesozoic granitic batholiths in the Jurassic arc-trench system in SW Japan are likely derived from the Cathaysian margin of South China (Fujisaki et al., 2014). Additionally, by compiling Sr-Nd isotopic composition of the Late Mesozoic to Cenozoic granitoids in SW Japan, Jahn (2010) concluded that most of the granitoids are similar to those in Cathaysia. Taken together, the SW Japanese Islands were thought to have affinity to the Cathaysian margin of South China. However, Hida of SW Japan belonged to the North China Craton in the north, and Oki belonged to the Yangtze Craton in the south (Fig. 8a; Barnes, 2003).

The geology and tectonic evolution of the Korean Peninsula have been thought to be closely related to the Chinese continent from the Archean to the present (Oh and Kusky, 2007; Rogers and Santosh, 2006; Zhai et al., 2007). The Hongseong Complex (HC) in the Gyeonggi Massif (GM) of the Korean Peninsula is likely an allochthon related to the Triassic collisional event like the Sulu Collisional Belt (Fig. 8b; Oh et al., 2005; Zhai et al., 2007). Hou et al. (2008) considered that a relatively complete Mesozoic collisional belt formed from the Imjingang Belt (IB) to the Okcheon Belt (OB), representing the eastward extension of the Sulu Collisional Belt on the Korean Peninsula (Fig. 8). Considering the coastal line similarity between the Korean Peninsula and Jiaodong Peninsula across the Huanghai Sea, we infer that the Korean Peninsula may have rift from the eastern Asian continental margin. The Jindo and Inchon of South Korea presumably correspond to Lianyungang and Rongcheng of China, respectively (Fig. 8b). The timing of the rifting/opening can be ascertained from the opening time of Bohai and Huanghai seas surrounded by Liaodong, Jiaodong, and Korean peninsulas, which needs further exploration.

On the basis of the data presented here together with the logical analysis following the work by Niu et al. (2015) and geological data in the literature, we have recently offered explicitly a testable hypothesis with illustrations on the origin of the Yellow Sea, i.e., "*The Yellow Sea is a continent-rifted basin with buried basaltic seafloor basement although the said seafloor spreading must have ceased for some time.*" (Niu and Tang, 2016). Fig. 8a is a further illustration on the concept and hypothesis discussed above. The insights we gain here point to urgent needs of plate tectonics reconstruction in the greater northwestern Pacific region since the Mesozoic.

### *5.4. Tectonic setting of Late Cretaceous-Paleocene magmatism in the eastern Asian continental margin*

The 97–56 Ma SAOB granitoids chemically belong to the high-K calc-alkaline series (Fig. 5a; Jahn et al., 2015). They are enriched in LREEs and LILEs, and depleted in HFSEs, consistent with being of subduction origin. The Late Cretaceous (97–88 Ma) granitoids, dacites and andesites in Tongjiang and Yanji areas of NE China with similar geochemical characteristics were interpreted to have formed in an active continental margin (Ji et al., 2007; Xu et al., 2013; Yu et al., 2013). Furthermore, the Late Cretaceous–Paleocene granitoids in the eastern Asian continent are restricted to the continental margin, i.e., the Russian Far East and NE China (97–56 Ma), the South Korea and SW Japan (96–71 Ma), and the South China (100–90 Ma). These granitoids and their spatial distribution are indirect but convincing evidence for the presence of the paleo-Pacific plate subduction beneath northeastern Asian continent in the Late Cretaceous–Paleocene.

It is generally accepted that the eastern Asian margin has experienced successive seafloor subduction with occasional oceanic ridge subduction since the Paleozoic (Isozaki, 1996; Isozaki et al., 2010; Maruyama et al., 1997). However, this successive subduction model poorly explained the magmatic hiatus (Menzies et al., 2007; Xu, 2001), continental-scale NW–SE shortening event (Charvet et al., 1994; Lapierre et al., 1997; Ratschbacher et al., 2003), and ubiquitous strike-slip features (Chen, 2000; Otsuki, 1992; Zhang et al., 2003; Zonenshain et al., 1990) in East Asia during the early Late Cretaceous (Yang, 2013). Therefore, Niu et al. (2015) proposed a logical hypothesis

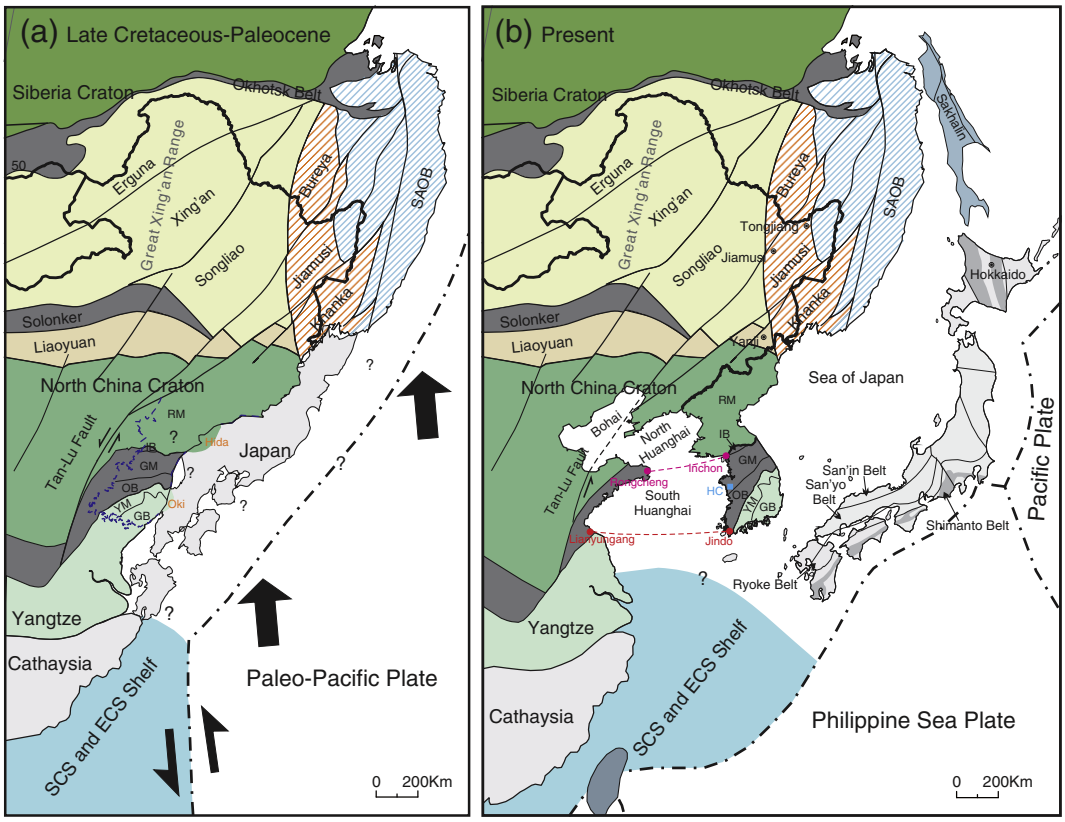


**Fig. 8.** (a) The Late Cretaceous-Paleocene paleogeographic reconstruction of the eastern Asian continental margin (modified from Niu et al., 2015; Sorokin et al., 2010a; Sun et al., 2013). The collision of the unsubductable mass of the paleo-Pacific plate (an oceanic plateau or micro-continent) at ~100 Ma jammed the trench located at the SE China coastal line, amalgamating to form the present-day East and South China Sea continental shelf of exotic origin (Niu et al., 2015). This event re-oriented the Pacific plate motion towards NNW and transformed its prior NW subduction boundary with eastern Asian continent into a transform boundary east of the continental shelf. This ended the granitoid magmatism on continental China at ~90 Ma (Niu et al., 2015), but oblique transform/subduction nature of the Sikhote-Alin Orogenic Belt and Korea-Japan to the north led to the continued granitoid for some time. The Russian Far East and NE China, Korea and Japan, and South China constituted the eastern Asian continental margin before the opening of the Huanghai, Bohai, and Japan seas. The blue dashed line represents the outline of the future Korea Peninsula. (b) The present-day geography of the eastern Asian continental margin. The red and pink dashed lines represent the tearing path of the Korean Peninsula from continental margin (modified from Niu et al., 2015; Sorokin et al., 2010a; Sun et al., 2013). RM = Rangnim Massif; GM = Gyeonggi Massif; YM = Yeongnam Massif; IB = Imjingang Belt; OB = Ogcheon Belt; GB = Gyeongsang Basin; HC = Hongseong Complex; SCS = South China Sea; and ECS = East China Sea. (For interpretation of the references to color in this figure legend, the reader is referred to the web version of this article.)

that the basement of the Chinese continental shelf (an exotic, buoyant and unsubductable mass) accreted to the southeastern continental China, hindering the further subduction of the paleo-Pacific plate. The termination of magmatism throughout the southeastern continental China at ~90 Ma indicates the cessation of crustal melting at this time. However, the interpreted mantle transition-zone slab dehydration would continue for some time (Niu et al., 2015). This trench jam was predicted to happen at ~100 Ma, and led to the re-orientation of the plate motion in the course of NNW direction as inferred from the age-progressive Emperor Seamount Chain of Hawaiian hotspot origin (its oldest unsubdued Meiji and Detroit seamounts are ~82 Ma), resulting in a transform contact between the NNW moving paleo-Pacific plate and eastern Asian continental plate east of the newly accreted Chinese continental shelf (Fig. 8a; Niu et al., 2015). However, the presence of the younger granitoids (<~90 Ma) in the SAOB and Korea-Japan area suggests that this same boundary to the north must be transpressional, allowing the NNW moving Pacific plate (Fig. 8a) to subduct obliquely beneath eastern Asian margin. Termination of the magmatism in South Korea and SW Japan at ~71 Ma suggests that the transpressional boundary may have evolved to true (?) transform contact by this time. We thus consider the Late Cretaceous-Paleocene magmatism in the Russian Far East, NE China, South Korea and SW Japan as a response to oblique subduction of the paleo-Pacific plate on an active continental margin.

In summary, though the trench jam resulted in a transform boundary between the paleo-Pacific plate and the newly accreted Chinese continental shelf, this same plate boundary may be transpressional in its northern segment with continued subduction component responsible for the younger (as young as ~56 Ma) granitoid magmatism (Fig. 8a).

It is worth noting that no Late Cretaceous-Paleocene magmatism is reported in NE Japan, showing magmatic discontinuity along the continental margin. Coincidentally, the Shimanto Belt, a Cretaceous accretionary complex, is also discontinuous between SW Japan and Hokkaido (Fig. 8b; Barnes, 2003). Presumably the eastern margin of NE Japan might have already been eroded into the trench by the subducting Pacific Plate. Different geological records in NE and SW Japan may be due to the fact that Japan is located at the junctions of four distinct plates (i.e. the Eurasian, Pacific, North American, and Philippine Sea plates). At present, the Pacific plate is subducting at a rate of 10 cm/yr beneath NE Japan, while the Philippine Sea plate is subducting at a rate of 4 cm/yr beneath SW Japan (Isozaki et al., 2010). The fast subduction of the Pacific plate may lead to the erosion rather than accretion along the NE Japan.

## 6. Conclusions

The major conclusions of this paper are as follows:

1. The primary magmas parental to the Late Cretaceous–Paleocene granitoids in the Sikhote-Alin Orogenic Belt were derived from partial melting of a juvenile lower crust accompanied by assimilation with ancient mature crust during magma ascent and evolution.

2. The zircon U-Pb ages of the Late Cretaceous–Paleocene granitoids in the Russian Far East and NE China, the South Korea and SW Japan, and the South China range from 97 Ma to 56 Ma, from 96 Ma to 71 Ma, and from 100 Ma to 90 Ma, respectively, showing that the magmatism ceased gradually from south to north.
3. Though the ~100 Ma trench jam resulted in a transform boundary between the paleo-Pacific plate and newly accreted Chinese continental shelf, this same plate boundary may be transpressional in its northern segment (the Russian Far East, NE China, South Korea and SW Japan) with continued oblique subduction, responsible for the younger granitoid magmatism.
4. The Russian Far East and NE China, Korea and Japan, and Chinese continental shelf constituted the eastern Asian continental margin before the opening of the Huanghai, Bohai and Japan seas, and their opening time and mechanism need to be further explored.
5. The plate tectonics configuration of the greater northwestern Pacific region we propose here is not a conclusion, but a logical hypothesis to be tested. The ways to test the hypothesis is given by Niu and Tang (2016) in the context of discussing the within-continent rift origin of the Yellow Sea.

Supplementary data to this article can be found online at doi:10.1016/j.lithos.2016.09.034.

## Acknowledgments

We thank the staff of the CUGW for their advice and assistance during U–Pb zircon dating analysis and the staff of the IGGCAS for help in the Hf isotope analysis. This work was financially supported by the National Natural Science Foundation of China (Grant 41330206), the National Key Basic Research Program of China (2013CB429803), the Opening Foundation of the State Key Laboratory of Geological Processes and Mineral Resources, China University of Geosciences (Wuhan) (GPMR201503), and a fellowship provided by the China Scholarship Council (201506170121).

## References

Amelin, Y., Lee, D.C., Halliday, A.N., 2000. Early–middle Archaean crustal evolution deduced from Lu–Hf and U–Pb isotopic studies of single zircon grains. Geochimica et Cosmochimica Acta 64, 4205–4225.
Anderson, T., 2002. Correction of common lead in U–Pb analyses that do not report $^{204}$Pb. Chemical Geology 192, 59–79.
Barnes, G.L., 2003. Origins of the Japanese Islands: the new "big picture". Nichibunken Japan Review 3–50.
Bouvier, A., Vervoort, J.D., Patchett, P.J., 2008. The Lu–Hf and Sm–Nd isotopic composition of CHUR: constraints from unequilibrated chondrites and implications for the bulk composition of terrestrial planets. Earth and Planetary Science Letters 273, 48–57.
Boynton, W.V., 1984. Geochemistry of the rare earth elements: meteorite studies. In: Henderson, P. (Ed.), Rare Earth Element Geochemistry. Elsevier, Amsterdam, pp. 63–114.
Chappell, B.W., 1999. Aluminium saturation in I- and S-type granites and the characterization of fractionated haplogranites. Lithos 46, 535–551.
Chappell, B.W., White, A.J.R., 1992. I-and S-type granites in the Lachlan Fold Belt. Geological Society of America Special Papers 272, 1–26.
Chappell, B.W., White, A.J.R., 2001. Two contrasting granite types: 25 years later. Australian Journal of Earth Sciences 48, 489–499.
Chappell, B.W., Bryant, C.J., Wyborn, D., 2012. Peraluminous I-type granites. Lithos 153, 142–153.
Charvet, J., Lapierre, H., Yu, Y., 1994. Geodynamic significance of the Mesozoic volcanism of southeastern China. Journal of Southeast Asian Earth Sciences 9, 387–396.
Chen, P., 2000. Paleoenvironmental changes during the Cretaceous in eastern China. In: Okada, H., Mateer, N.J. (Eds.), Cretaceous Environments of Asia. Elsevier Science, pp. 81–90.
Elliott, T., 2003. Tracers of the slab. Inside the subduction factory, pp. 23–45.
Faure, M., Natal'in, B., 1992. The geodynamic evolution of the eastern Eurasian margin in Mesozoic times. Tectonophysics 208 (4), 397–411.
Fujisaki, W., Isozaki, Y., Maki, K., Sakata, S., Hirata, T., Maruyama, S., 2014. Age spectra of detrital zircon of the Jurassic clastic rocks of the Mino-Tanba AC belt in SW Japan: constraints to the provenance of the mid-Mesozoic trench in East Asia. Journal of Asian Earth Sciences 88, 62–73.
Gonevchuk, V.G., Gonevchuk, G.A., Korostelev, P.G., Semenyak, B.I., Seltmann, R., 2010. Tin deposits of the Sikhote-Alin and adjacent areas (Russian Far East) and their magmatic association. Australian Journal of Earth Sciences 57 (6), 777–802.
Grebennikov, A.V., Popov, V.K., 2014. Petrochemical aspects of the Late Cretaceous and Paleogene igmimbrite volcanism of East Sikhote-Alin. Russian Journal of Pacific Geology 8 (1), 38–55.
Griffin, W.L., Pearson, N.J., Belousova, E., Jackson, S.E., Achterbergh, E., Reilly, S.Y., Shee, S.R., 2000. The Hf isotope composition of cratonic mantle: LAM-MC-ICPMS analysis of zircon megacrysts in kimberlites. Geochimica et Cosmochimica Acta 64, 133–147.
Herzig, C.T., Kimbrough, D.L., Tainosho, Y., Kagami, H., Iizumi, S., Hayasaka, Y., 1998. Late Cretaceous U/Pb zircon ages and Precambrian crustal inheritance in Ryoke granitoids, Kinki and Yanai districts, Japan. Geochemical Journal 32, 21–32.
Hirose, K., 1997. Melting experiments on lherzolite KLB-1 under hydrous conditions and generation of high-magnesian andesitic melts. Geology 25, 42–44.
Hou, Q.L., Wu, Y.D., Wu, F.Y., Zhai, M.G., Guo, J.H., Li, Z., 2008. Possible tectonic manifestations of the Dabie-Sulu orogenic belt on the Korean Peninsula. Geological Bulletin of China 27 (10), 1659–1666 (in Chinese with English abstract).
Hwang, B.H., 2011. Timing of granitic magma mixing in the southeastern Gyeongsang Basin, Korea: SHRIMP-RG zircon data. International Geology Review 53 (10), 1150–1162.
Imaoka, T., Nakashima, K., Kamei, A., Hayasaka, Y., Ogita, Y., Ikawa, T., Itaya, T., Takahashi, Y., Kagami, H., 2014. Anatomy of the Cretaceous Hobenzan pluton, SW Japan: internal structure of a small zoned pluton, and its genesis. Lithos 208, 81–103.
Irvine, T.H., Baragar, W.R.A., 1971. A guide to the chemical classification of the common volcanic rocks. Canadian Journal of Earth Sciences 8, 523–548.
Isozaki, Y., 1996. Anatomy and genesis of a subduction-related orogen: a new view of geotectonic subdivision and evolution of the Japanese Islands. Island Arc 5, 289–320.
Isozaki, Y., Aoki, K., Nakama, T., Yanai, S., 2010. New insight into a subduction-related orogen: a reappraisal of the geotectonic framework and evolution of the Japanese Islands. Gondwana Research 18 (1), 82–105.
Jahn, B.M., 2010. Accretionary orogeny and evolution of the Japanese Island-implication from a Sr-Nd isotopic study of the Phanerozoic granitoids from SW Japan. American Journal of Science 310 (10), 1210–1249.
Jahn, B.M., Valui, G., Kruk, N., Gonevchuk, V., Usuki, M., Wu, J.T., 2015. Emplacement ages, geochemical and Sr–Nd–Hf isotopic characterization of Mesozoic to early Cenozoic granitoids of the Sikhote-Alin Orogenic Belt, Russian Far East: crustal growth and regional tectonic evolution. Journal of Asian Earth Sciences 111, 872–918.
Ji, W.Q., Xu, W.L., Yang, D.B., Pei, F.P., Jin, K., Liu, X.M., 2007. Chronology and geochemistry of volcanic rocks in the Cretaceous Suifenhe formation in eastern Heilongjiang, China. Acta Geologica Sinica (English edition) 81 (2), 266–277.
Khanchuk, A.I., 2001. Pre-Neogene tectonics of the sea-of-Japan region: a view from the Russian side. Earth Science (Chikyu Kagaku) 55, 275–291.
Kiminami, K., Imaoka, T., 2013. Spatiotemporal variations of Jurassic–Cretaceous magmatism in eastern Asia (Tan–Lu Fault to SW Japan): evidence for flat–slab subduction and slab rollback. Terra Nova 25 (5), 414–422.
Koschek, G., 1993. Origin and significance of the SEM cathodoluminescence from zircon. Journal of Microscopy 171, 223–232.
Kotov, A.B., Velikoslavinskii, S.D., Sorokin, A.A., Kotova, L.N., Sorokin, A.P., Larin, A.M., Kovach, V.P., Zagornaya, N.Y., Kurguzova, A.V., 2009. Age of the Amur group of the Bureya-Jiamusi Superterrane in the Central Asian Fold Belt: Sm–Nd isotope evidence. Doklady Earth Sciences 429, 1245–1248.
Kruk, N.N., Simanenko, V.P., Gvozdev, V.I., Golozubov, V.V., Kovach, V.P., Serov, P.I., Kholodnov, V.V., Moskalenko, E.Y., Kuibida, M.L., 2014. Early Cretaceous granitoids of the Samarka terrane (Sikhote-Alin'): geochemistry and sources of melts. Russian Geology and Geophysics 55 (2), 216–236.
Kushiro, I., Syono, Y., Akimoto, S., 1968. Melting of a peridotite nodule at high pressures and high water pressures. Geophysical Research 73, 6023–6029.
Lapierre, H., Jahn, B.M., Charvet, J., Yu, Y.W., 1997. Mesozoic magmatism in Zhejiang Province and its relation with the tectonic activities in SE China. Tectonophysics 274, 321–338.
Lee, Y.S., Ishikawa, N., Kim, W.K., 1999. Paleomagnetism of Tertiary rocks on the Korean Peninsula: tectonic implications for the opening of the East Sea (Sea of Japan). Tectonophysics 304 (1), 131–149.
Li, W.M., Takasu, A., Liu, Y.J., Guo, X.Z., 2010. Newly discovered garnet–barroisite schists from the Heilongjiang complex in the Jiamusi Massif, northeastern China. Journal of Mineralogical and Petrological Sciences 105, 86–91.
Liu, Y.S., Hu, Z.C., Gao, S., Günther, D., Xu, J., Gao, C.G., Chen, H.H., 2008. In situ analysis of major and trace elements of anhydrous minerals by LA-ICP-MS without applying an internal standard. Chemical Geology 257, 34–43.
Liu, Y.S., Gao, S., Hu, Z.C., Gao, C.G., Zong, K.Q., Wang, D.B., 2010. Continental and oceanic crust recycling-induced melt-peridotite interactions in the trans-North China orogen: U–Pb dating, Hf isotopes and trace elements in zircons of mantle xenoliths. Journal of Petrology 51, 537–571.
Ludwig, K.R., 2003. ISOPLOT 3: a geochronological toolkit for microsoft excel. Berkeley Geochronology Centre Special Publication 4, p. 74.
Malinovsky, A.I., Golozubov, V.V., 2011. Lithology and depositional settings of the terrigenous sediments along transform plate boundaries: evidence from the early cretaceous Zhuravlevka terrane in Southern Sikhote Alin. Russian Journal of Pacific Geology 5 (5), 400–417.
Maniar, P.D., Piccoli, P.M., 1989. Tectonic discrimination of granitoids. Geological Society of America Bulletin 101 (5), 635–643.
Maruyama, S., Isozaki, Y., Kimura, G., Terabayashi, M., 1997. Paleogeographic maps of the Japanese Islands: plate tectonic synthesis from 750 Ma to the present. Island Arc 6, 121–142.
Menzies, M., Xu, Y., Zhang, H., Fan, W., 2007. Integration of geology, geophysics and geochemistry: a key to understanding the North China Craton. Lithos 96, 1–21.
Nakajima, T., Kamiyama, H., Williams, I.S., Tani, K., 2004. Mafic rocks from the Ryoke Belt, southwest Japan: implications for Cretaceous Ryoke/San-yo granitic magma genesis. Geological Society of America Special Papers 389, 249–263.

Niu, Y.L., 2005. Generation and evolution of basaltic magmas: some basic concepts and a new view on the origin of Mesozoic–Cenozoic basaltic volcanism in eastern China. Geological Journal of China Universities 11 (1), 9–46.
Niu, Y.L., Tang, J., 2016. Origin of the Yellow Sea: an insight. Science Bulletin 61, 1076–1080.
Niu, Y.L., Zhao, Z.D., Zhu, D.C., Mo, X.X., 2013. Continental collision zones are primary sites for net continental crust growth – a testable hypothesis. Earth-Science Reviews 127, 96–110.
Niu, Y.L., Liu, Y., Xue, Q.Q., Shao, F.L., Chen, S., Duan, M., Guo, P.Y., Gong, H.M., Hu, Y., Hu, Z.X., Kong, J.J., Li, J.Y., Liu, J.J., Sun, P., Sun, W.L., Ye, L., Xiao, Y.Y., Zhang, Y., 2015. Exotic origin of the Chinese continental shelf: new insights into the tectonic evolution of the western Pacific and eastern China since the Mesozoic. Science Bulletin 60, 1598–1616.
Nowell, G.M., Kempton, P.D., Noble, S.R., Fitton, J.G., Saunders, A.D., Mahoney, J.J., Taylor, R.N., 1998. High precision Hf isotope measurements of MORB and OIB by thermal ionization mass spectrometry: insights into the depleted mantle. Chemical Geology 149, 211–233.
Oh, C.W., Kusky, T., 2007. The Late Permian to Triassic Hongseong-Odesan collision belt in South Korea, and its tectonic correlation with China and Japan. International Geology Review 49 (7), 636–657.
Oh, C.W., Choi, S.G., Zhai, M.G., Guo, J.H., Jin, Y.Y., 2005. First finding of eclogite facies metamorphic event in South Korea and its correlation with the Dabie–Sulu collision belt in China. Journal of Geology 113, 226–232.
O'Hara, M.J., 1965. Primary magmas and the origin of basalts. Scottish Journal of Geology 1 (1), 19–40.
Otofuji, Y.I., 1996. Large tectonic movement of the Japan Arc in late Cenozoic times inferred from paleomagnetism: review and synthesis. Island Arc 5, 229–249.
Otofuji, Y., Hayashida, A., Torii, M., 1985. When was the Japan Sea opened? Paleomagnetic evidences for Southwest Japan. In: Nasu, N., Uyeda, S., Kushiro, I., Kobayashi, K., Kagami, H. (Eds.), Formation of Active Ocean Margins. Terrapub, Tokyo, pp. 551–566.
Otsuki, K., 1992. Oblique subduction, collision of microcontinents and subduction of oceanic ridge: their implications on the Cretaceous tectonics of Japan. Island Arc 1, 51–63.
Peccerillo, A., Taylor, A.R., 1976. Geochemistry of Eocene calc-alkaline volcanic rocks from the Kastamonu area, Northern Turkey. Contributions to Mineralogy and Petrology 58 (1), 63–81.
Pupin, J.P., 1980. Zircon and granite petrology. Contributions to Mineralogy and Petrology 73 (3), 207–220.
Ratschbacher, L., Hacker, B.R., Calvert, A., Webb, L.E., Grimmer, J.C., McWilliams, M.O., Ireland, T., Dong, S., Hu, J., 2003. Tectonics of the Qinling (Central China): tectonostratigraphy, geochronology, and deformation history. Tectonophysics 366, 1–53.
Rogers, J.J.W., Santosh, M., 2006. The Sino-Korea Craton and supercontinent history: problems and perspectives. Gondwana Research 9, 21–23.
Simanenko, V.P., Khanchuk, A.I., Golozoubov, V.V., 2002. The first data on geochemistry of Albian-Cenomanian volcanism in the Southern Primorye, Russian Far East. Geochemistry International C/C of Geokhimiia 40, 86–90.
Sorokin, A.A., Ponomarchuk, V.A., Derbeko, I.M., Sorokin, A.P., 2005. $^{40}Ar/^{39}Ar$ geochronology and geochemical characteristics of Mesozoic igneous complexes in the Khingan–Olonoi volcanic zone (Far East). Stratigraphy and Geological Correlation 13 (3), 276–290.
Sorokin, A.A., Sorokin, A.P., Ponomarchuk, V.A., Travin, A.V., Melnikova, O.V., 2009. Late Mesozoic volcanism of the eastern part of the Argun superterrane (Far East): geochemistry and $^{40}Ar/^{39}Ar$ geochronology. Stratigraphy and Geological Correlation 17 (6), 645–658.
Sorokin, A.A., Kotov, A.B., Sal'nikova, E.B., Kudryashov, N.M., Anisimova, I.V., Yakovleva, S.Z., Fedoseenko, A.M., 2010a. Granitoids of the Tyrma–Bureya complex in the northern Bureya-Jiamusi superterrane of the Central Asian fold belt: age and geodynamic setting. Russian Geology and Geophysics 51, 563–571.
Sorokin, A.A., Sorokin, A.P., Ponomarchuk, V.A., Travin, A.V., 2010b. The age and geochemistry of volcanic rocks on the eastern flank of the Umlekan–Ogodzha volcanoplutonic belt (Amur region). Russian Geology and Geophysics 51 (4), 369–379.
Sun, S.S., McDonough, W.F., 1989. Chemical and isotopic systematics of ocneanic basalts: implications for mantle composition and processes. In: Saunders, A.D., Norry, M.J. (Eds.), Magmatism in Ocean Basins. Geological Society of Special Publication, London, pp. 313–345.
Sun, M.D., Chen, H.L., Zhang, F.Q., Wilde, S.A., Dong, C.W., Yang, S.F., 2013. A 100 Ma bimodal composite dyke complex in the Jiamusi block, NE China: an indication for lithospheric extension driven by paleo-Pacific roll-back. Lithos 162, 317–330.
Utkin, V.P., 1980. Fault Displacements and Their Research Procedure. Nauka, Moscow (144 pp.).
Vervoort, J.D., Plank, T., Prytulak, J., 2011. The Hf = Nd isotopic composition of marine sediments. Geochimica et Cosmochimica Acta 75, 5903–5926.
Wilson, M., 1991. Igneous Petrogenesis: A Global Tectonic Approach. Harper Collins Academic, pp. 1–466.
Wu, G., Sun, F.Y., Zhao, C.S., Li, Z.T., Zhao, A.L., Pang, Q.B., Li, G.Y., 2005. Discovery of the Early Paleozoic post-collisional granites in northern margin of the Erguna massif and its geological significance. Chinese Science Bulletin 50, 2733–2743.
Wu, F.Y., Yang, Y.H., Xie, L.W., Yang, J.H., Xu, P., 2006. Hf isotopic compositions of the standard zircons and baddeleyites used in U–Pb geochronology. Chemical Geology 234, 105–126.
Wu, F.Y., Sun, D.Y., Ge, W.C., Zhang, Y.B., Grant, M.L., Wilde, S.A., Jahn, B.M., 2011. Geochronology of the Phanerozoic granitoids in northeastern China. Journal of Asian Earth Sciences 41, 1–30.
Xu, Y.G., 2001. Thermo-tectonic destruction of the Archean lithospheric keel beneath the Sino-Korean Craton in China: evidence, timing and mechanism. Physics and Chemistry of the Earth 26, 747–757.
Xu, W.L., Pei, F.P., Wang, F., Meng, E., Ji, W.Q., Yang, D.B., Wang, W., 2013. Spatial–temporal relationships of Mesozoic volcanic rocks in NE China: constraints on tectonic overprinting and transformations between multiple tectonic regimes. Journal of Asian Earth Sciences 74, 167–193.
Yang, Y.T., 2013. An unrecognized major collision of the Okhotomorsk Block with East Asia during the Late Cretaceous, constraints on the plate reorganization of the Northwest Pacific. Earth-Science Reviews 126 (11), 96–115.
Yang, J.H., Wu, F.Y., Shao, J., Simon, A.W., Xie, L.W., Liu, X.M., 2006. Constraints on the timing of uplift of the Yanshan Fold and Thrust Belt, North China. Earth and Planetary Science Letters 246, 245–336.
Yu, X., Xiao, J., Chen, H.L., Zhang, F.Q., Xu, Y., Dong, C.W., Pang, Y.M., 2008. Phanerozoic magmatic events in the basement of Songliao basin: SHRIMP dating of captured zircons from Ying Clemens Formation volcanic rocks. Acta Petrologica Sinica 24, 1123–1130 (in Chinese with English abstract).
Yu, J.J., Zhang, Y.L., Ge, W.C., Yang, H., 2013. Geochronology and geochemistry of the Late Cretaceous granitoids in the northern margin of the Sanjiang basin, NE China and its tectonic implications. Acta Petrologica Sinica 29 (2), 369–385 (in Chinese with English abstract).
Yuan, H.L., Gao, S., Liu, X.M., Li, H.M., Günther, D., Wu, F.Z., 2004. Accurate U–Pb age and trace element determinations of zircon by laser ablation inductively coupled plasma mass spectrometry. Geostandard Newsletter 28, 353–370.
Zen, E.A., 1986. Aluminium enrichment in silicate melts by fractional crystallization: some mineralogic and petrographic constraints. Journal of Petrology 27, 1095–1117.
Zhai, M.G., Guo, J.H., Li, Z., Chen, D.Z., Peng, P., Li, T.S., Hou, Q.L., Fan, Q.C., 2007. Linking the Sulu UHP belt to the Korean Peninsula: evidence from eclogite, Precambrian basement, and Paleozoic sedimentary basins. Gondwana Research 12 (4), 388–403.
Zhang, Y., Dong, S., Shi, W., 2003. Cretaceous deformation history of the middle Tan-Lu fault zone in the Shandong Province, eastern China. Tectonophysics 363, 243–258.
Zhang, Y.B., Zhai, M., Hou, Q.L., Li, T.S., Liu, F., Hu, B., 2012. Late Cretaceous volcanic rocks and associated granites in Gyeongsang Basin, SE Korea: their chronological ages and tectonic implications for cratonic destruction of the North China Craton. Journal of Asian Earth Sciences 47, 252–264.
Zhou, J.B., Wilde, S.A., Zhang, X.Z., Ren, S.M., Zheng, C.Q., 2011. Early Paleozoic metamorphic rocks of the Erguna block in the Great Xing'an range, NE China: evidence for the timing of magmatic and metamorphic events and their tectonic implications. Tectonophysics 499, 105–117.
Zonenshain, L.P., Kuzmin, M.I., Natapov, L.M., 1990. Geology of the USSR: a plate tectonic synthesis. Geodynamic Series American Geophysical Union 21, 1–242.